JOURNAL OF MATERIALS SCIENCE 33 (1998) 4531–4541

Microstructure and tribological properties of alumina ceramic with laser-dispersed tungsten additions

K. PRZEMECK, K.-H. ZUM GAHR
University of Karlsruhe, Institute of Materials Science II, and Forschungszentrum Karlsruhe, Institute of Materials Research I, Karlsruhe, Germany
E-mail: zumgahr@imf.fzk.de

The surface of slightly porous, commercially available alumina ceramic was laser-modified with tungsten and/or zirconia additions. The thickness of the resulting multiphase surface layers ranged from 300–800 μm depending on the chemical composition and the parameters of the laser process used. Microstructure and worn surfaces were analysed by scanning electron microscopy and energy- dispersive X-ray spectroscopy. Mechanical properties were characterized by using Vickers hardness and nanoindentor testing. Tribological tests were carried out on the surface-modified ceramics using a ball-on-block tribometer. All tests were conducted in unlubricated oscillating sliding contact against balls of alumina in laboratory air at room temperature, relative humidities varying between 3% and 80%, and in distilled water. The multiphase surface layers showed a total volume fraction of second phases up to 40 vol% embedded in the alumina matrix, whereas the average size of the alumina grains was substantially reduced compared with the substrate ceramic. Tungsten dispersoids were distributed homogenously in the ceramic matrix and eutectic Al_2O_3–ZrO_2 phase occurred along the boundaries of the alumina crystallites. Mechanical and tribological properties varied as a function of the microstructure of the laser-modified ceramics, i.e. type and volume fraction of the second phases, and both friction and wear were substantially reduced compared with the commercially available monolithic alumina ceramic used for reference. Friction coefficient and amount of linear wear of the ceramics decreased with increasing relative humidity of the surrounding air. © *1998 Kluwer Academic Publishers*

1. Introduction

Advanced alumina ceramics were used for components with tribological, mechanical, chemical and thermal requirements such as seal rings, drawn cones, guides or bearing parts. Favourable properties of alumina for these applications are high stiffness and hardness, temperature stability, corrosion and wear resistance, as well as low density. However, monolithic alumina can suffer severe problems under very high tribological and/or mechanical loads, owing to its inherent brittleness and lack of defect tolerance which can result in low wear resistance and relatively high friction coefficients in self-mated unlubricated sliding contact. Tribological properties of monolithic alumina ceramic are characterized by a transition from mild to severe wear, owing to a change of mechanism from predominantly tribochemical reactions to surface damage by microfracture, which results in spalling of individual grains or parts of them, abrasion and formation of surface layers consisting of compacted wear debris. This transition is influenced by microstructural parameters, such as size and shape of grains, porosity and/or second phases but also by environmental conditions, e.g. humidity, and operating parameters as sliding velocity, temperature and load [1–3]. Hence, it is concluded that microstructural modifications resulting in enhanced fracture toughness, for example, can lead to improved tribological performance of alumina [4–6]. All tribologically induced interactions between two solids mated in sliding contact are concentrated on a relatively thin surface zone. Therefore, it may be sufficient and economical to modify the microstructure in a surface zone of a thickness of a few hundred micrometres only.

Recent studies [7–9] showed that CO_2-laser radiation can be successfully used for producing multiphase surface zones of thicknesses between about 100 and 300 μm on alumina by embedding oxides, nitrides, borides or carbides which resulted in substantially improved tribological properties compared with those of monolithic alumina. Ductile metallic phases embedded in brittle ceramics offer a high potential for increased fracture toughness [10–13] and it can be assumed that metallic phases may also improve the tribological properties by avoiding intercrystalline

microcracking in the contact area under high applied loads.

The aim of the present work was to study the tribological behaviour of surface-modified alumina ceramics which were produced by using CO_2-laser irradiation. The multiphase surface structures consisted of an alumina matrix in which tungsten dispersoids and eutectic alumina–zirconia phases were embedded. Tribological properties were investigated during oscillating sliding contact against alumina balls using a ball-on-block tribometer at different relative humidities in laboratory air and distilled water, respectively.

2. Experimental procedure

2.1. Materials and laser processing

Laser-induced surface treatment was conducted on a commercially available Al_2O_3 ceramic (Al24, Fa. Friatec) with less than 5 vol% open porosity. Properties of the received Al_2O_3 ceramic Al24 and the Al_2O_3 ceramics laser modified by adding tungsten (Al24W), unstabilized ZrO_2 (Al24Z) and both tungsten and ZrO_2 (Al24WZ), respectively, are listed in Table I. Further, a dense, monolithic Al_2O_3 ceramic (Al23, Fa. Friatec) was included in the investigations for reference.

For microstructural modification (Al24Z, Al24WZ), the as-received Al_2O_3 ceramic Al24 was precoated with a suspension consisting of zirconia powder with an average particle size of 1.3 μm and isopropyl alcohol. The coating with a thickness of 40 μm was dried at room temperature and then heated up and held at 500 °C for 1 h. Additional information is given elsewhere [7].

Before laser treatment, the precoated (Al24Z, Al24WZ) or uncoated (Al24W) specimens, respectively, were preheated to 1500 °C in laboratory air using a heating rate of 10 K min^{-1}, and were held at this temperature for at least 30 min. In order to reduce heat loss during laser treatment, the specimens were placed on a brick of porous alumina. Surface melting was produced on the specimens using a high-power CO_2 laser with a beam integrator which generated a rectangular beam cross-section of 1×6 mm^2 (Fig. 1a). Laser treatment was carried out on surface strips of 6 mm width at an average power range between 200 and 220 W and a traverse speed of 250 mm min^{-1}. A commercial powder feeder was used for processing of the ceramics Al24W and Al24WZ to convey the tungsten powder (with an average particle size of 7 μm) to the injection nozzle and a special support was constructed allowing the accurate adjustment of the injection nozzle to the laser beam. After laser treatment, specimens were deposited in an argon gas-flooded chamber to prevent oxidation during cooling.

Microstructures of the ceramics and worn surfaces were analysed using standard ceramographic techniques, scanning electron microscopy (SEM) and energy-dispersive X-ray spectroscopy (EDX). Mechanical properties of the monolithic alumina ceramic Al23 and the laser-modified ceramics were characterized by Vickers hardness HV_{500} testing, determination of indentation fracture toughness K^*_{1c} (Vickers diamond indentor) [14], and calculating of Young's modulus from the slope of the load–indentation curves from nanoindentor testing [15].

2.2. Tribological test

Before oscillating sliding wear tests, all block specimens were ground and polished to an average surface roughness of R_a (c.l.a.) $\leqslant 0.1$ μm. Grinding procedure led to a surface removal of about 80–150 μm thickness. Tribological properties were measured in a ball-on-block tribometer (Fig. 1c, Optimol SRV) under conditions of unlubricated, oscillating sliding contact. High-density Al_2O_3 balls (F 99.7, diameter = 10 mm, Fa. Friatec) were used as counterbodies with surface roughness of $R_a \leqslant 0.1$ μm, average grain size of 9 μm and hardness of 1700 HV_{500}. The tests were run at a constant normal load of 40 N, a frequency of oscillation of 20 Hz and a stroke of 0.5 mm, which resulted in an average sliding speed of 0.02 m s^{-1}. The number of 1.44×10^5 oscillation cycles led to a total wear path of 0.144 km. All tribological tests were carried out at room temperature (25–30 °C) inside a climate chamber in which the relative humidity (RH) was adjusted to values of 3%, 30%, 50% and 80%, respectively, by rinsing with dry or wet air. In further tests, distilled water was added to the contact area between ball and block using a feeding rate of 0.1 ml and every 20 min.

During each test, friction force and amount of total linear wear, W_1 (sum of ball and block wear), were

TABLE I Materials, additives and microstructural parameters of the monolithic Al_2O_3 ceramics in the received condition (Al23, Al24), the laser surface-modified ceramics (Al24W, Al24Z and Al24WZ) and the Al_2O_3 balls (F 99.7) used as counterbodies in the tribological tests

	Material					
	Al23	Al24	Al24W	Al24Z	Al24WZ	F 99.7 (ball)
Additive	–	–	W	ZrO_2	W + ZrO_2	–
Al_2O_3-matrix, (vol %)	100	100	75–80	85	58–62	100
Grain-boundary phase (vol %)	–	–	–	15	20	–
W-dispersoid (vol %)	–	–	20–25	–	18–22	–
Average Al_2O_3 grain size (μm)	6.5	30	20	10	6	9
Open porosity (vol %)	0	<5	<2	≈ 0	≈ 0	0

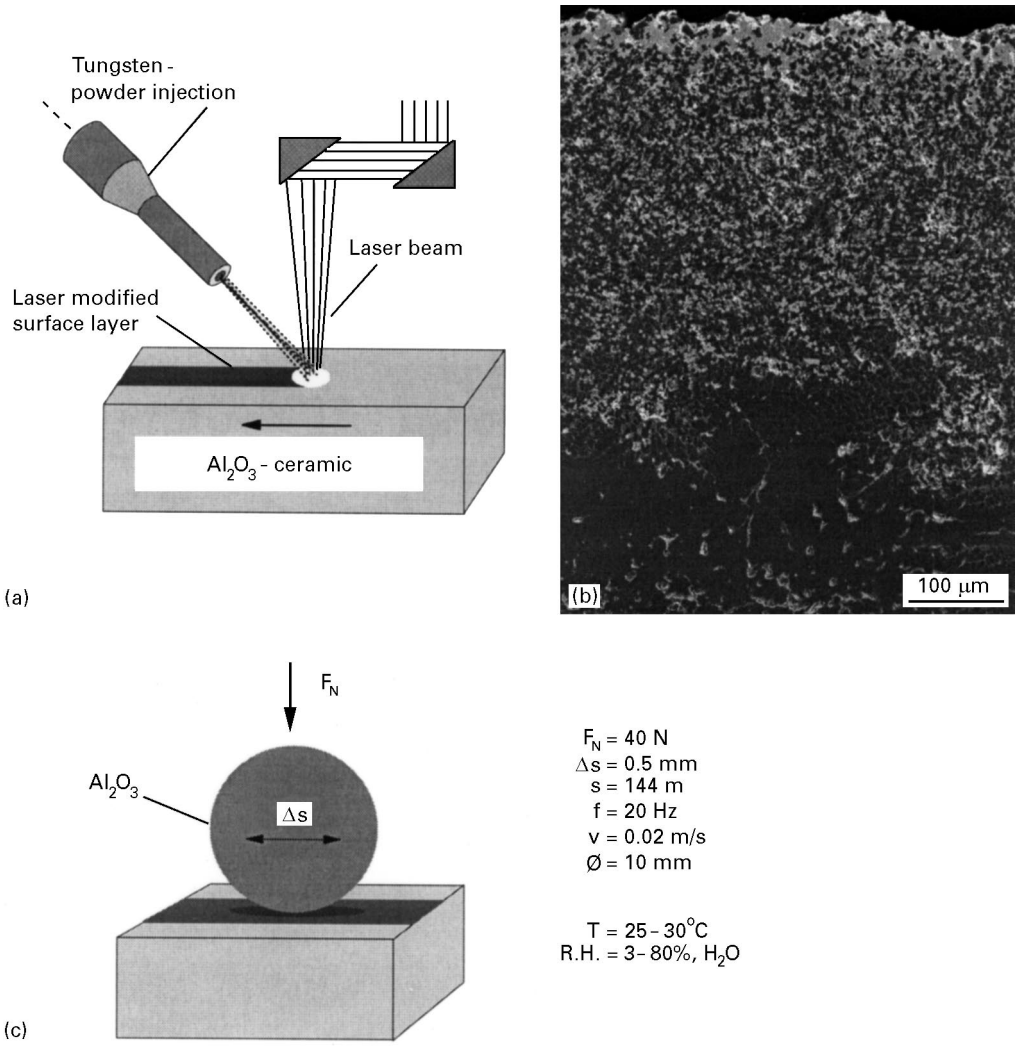

Figure 1 (a) Experimental set-up for laser treatment, (b) scanning electron micrograph of a cross-section through the surface-modified ceramic Al24WZ perpendicular to the travel direction of the laser beam, and (c) the tribological system ball-on-block used in oscillating sliding wear tests.

measured continuously. After the tests, linear wear W_l^* of the balls and the blocks was separately determined from surface profiles recorded with a stylus profilometer. Friction coefficients reported were calculated from the stationary values after a short period of running-in. All tribological results presented are average values of at least two individual tests.

3. Results

3.1. Microstructure

Fig. 2 shows scanning electron micrographs of the dense alumina ceramic Al23 used for reference and three different laser-modified ceramics. According to Table I, the monolithic ceramic Al23 (Fig. 2a) displayed an average grain size of 6.5 μm and no open porosity. In comparison, the as-delivered ceramic Al24, which was used as substrate material for laser treatment, contained an open porosity of less than 5 vol% and an average grain size of about 30 μm.

Laser treatment led to multiphase surface layers with a thickness between 300 and 800 μm, depending on the added constituents and process parameters used (Fig. 1b). The average size of alumina crystallites in the multiphase microstructures depended on chemical composition (Fig. 2b–d) and was reduced up to a factor of about 5 compared with the as-received substrate ceramic Al24 (Table I). All laser-modified ceramics showed locally columnar grains with lengths up to about 30 μm. Microstructure of the ceramic Al24W (Fig. 2b) contained tungsten dispersoids which were homogeneously distributed in the alumina matrix. A content of 20–25 vol% irregularly shaped metallic particles was measured at an average particle size of about 7 μm. Only a slight amount of porosity (< 2 vol%) was observed in the alumina matrix.

Laser remelting of ZrO_2-precoated alumina Al24Z (Fig. 2c) and Al24WZ with injection of tungsten (Fig. 2d) resulted in dense surface layers exhibiting the smallest size of alumina crystallites. A fine lamellar eutectic Al_2O_3–ZrO_2 phase occurred along the grain boundaries of the Al_2O_3 matrix and its content was measured to 15 or 20 vol% in the ceramic Al24Z and Al24WZ, respectively. Tungsten particles of a volume fraction between 18% and 22% were distributed homogeneously in the grain-boundary phase and Al_2O_3 crystallites with the ceramic Al24WZ. Laser alloying

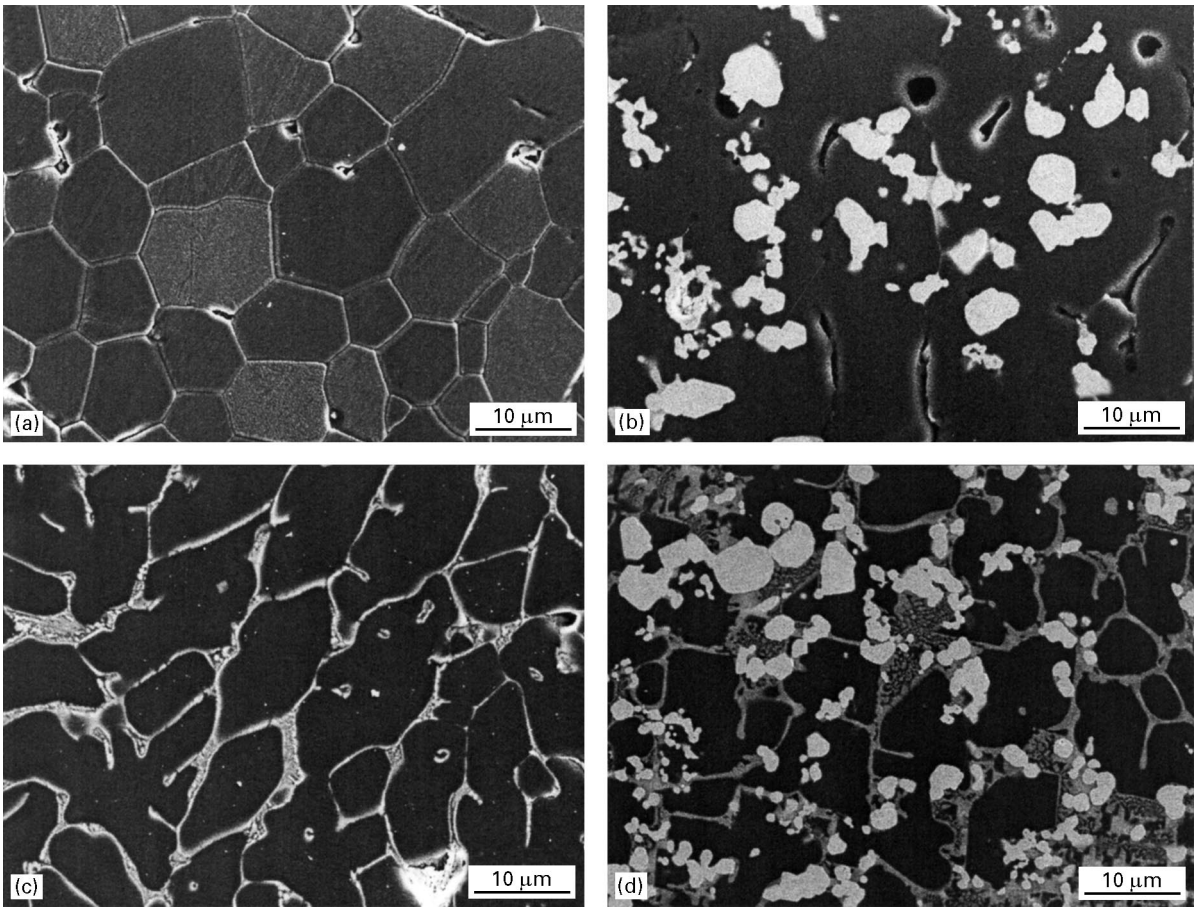

Figure 2 Scanning electron micrographs of (a) the monolithic alumina ceramic Al23, and the surface-modified ceramics (b) Al24W, (c) Al24Z, and (d) Al24WZ, respectively.

of alumina ceramic by ZrO_2 powder-precoating (Al24Z) led to surface layers showing a tendency to form crack networks due to thermally induced stresses during cooling procedure, which could be reduced by preheating conditions and optimized laser parameters [7]. Crack networks did not occur in the tungsten-containing ceramics (Al24W, Al24WZ) and only a few cracks were detected in the transition area between the composite surface layer and the underlying non-melted substrate ceramic. A well-adjusted position of the powder nozzle to the melt bath (Fig. 1a) was important for obtaining dense surface layers without crack networks.

Table II shows values of hardness, fracture toughness, K^*_{1c}, and Young's modulus of the monolithic alumina Al23 compared with the surface-modified Al24W, Al24Z and Al24WZ ceramics, respectively. Hardness was markedly reduced by adding tungsten dispersoids (1400 HV_{500} for Al24W) or alloying with ZrO_2 (1550 HV_{500} for Al24Z) compared with the reference alumina Al23 (2000 HV_{500}). Al24WZ containing a total volume fraction of second phases of about 40% resulted in an average hardness value of only 1250 HV_{500}.

Vickers hardness testing (HV_{500}) led to surface cracks on all investigated ceramics at the corners of the indentations. Tungsten dispersoids in the alumina matrix (Al24W) slightly increased the fracture toughness (Table II), compared with the reference ceramic Al23, mainly by crack deflection. The highest values of K^*_{1c} were measured in the surface of Al24WZ, whereas fracture toughness was more than 35% greater than that of Al23 owing to crack deflection at tungsten particles and the effect of the eutectic Al_2O_3–ZrO_2 grain-boundary phase on crack formation and propagation.

Young's modulus calculated from load–indentation curves showed lower values on surfaces of the laser-modified ceramics than on the monolithic ceramic Al23 (Table II). Only a slightly lower value was measured on the ZrO_2 laser-alloyed ceramic (Al24Z) containing 15 vol% eutectic grain-boundary phase, while Young's modulus on the ceramic Al24WZ with about 40 vol% second phases showed a substantially lower (35%) value of 260 GPa.

3.2. Oscillating sliding wear

3.2.1. Effect of microstructure

Tribological tests were conducted on the laser-modified ceramics Al24W, Al24Z and Al24WZ in unlubricated oscillating sliding contact (Fig. 1c) against Al_2O_3-balls (F 99.7) at a relative humidity of 50% in air. After a short period of running-in, the friction coefficient increased sharply on the ceramics Al23 and Al24W (Fig. 3a) to a maximum value between 0.9 and 1.1 before it decreased continuously to quasi-stationary values of 0.6 (Al24W) and 0.7 (Al23), respectively,

TABLE II Hardness HV_{500}, fracture toughness K^*_{Ic} and Young's modulus of the monolithic alumina ceramics Al23 and F 99.7 as well as of the laser-modified ceramics Al24W, Al24Z and Al24WZ. p_{max} is the maximum Hertzian contact pressure applied to the ceramics when mated to the ceramic F99.7 balls

	Material				
	Al23	Al24W	Al24Z	Al24WZ	F 99.7 (ball)
Hardness, HV_{500}	2000	1400	1550	1250	1700
Fracture toughness K^*_{Ic} (MPa $m^{1/2}$)	3.6	3.8	4.2	4.9	3.5
Young's modulus, (GPa)	400	275	380	260	380
Hertzian pressure p_{max} (MPa)	1502	1315	1477	1286	–

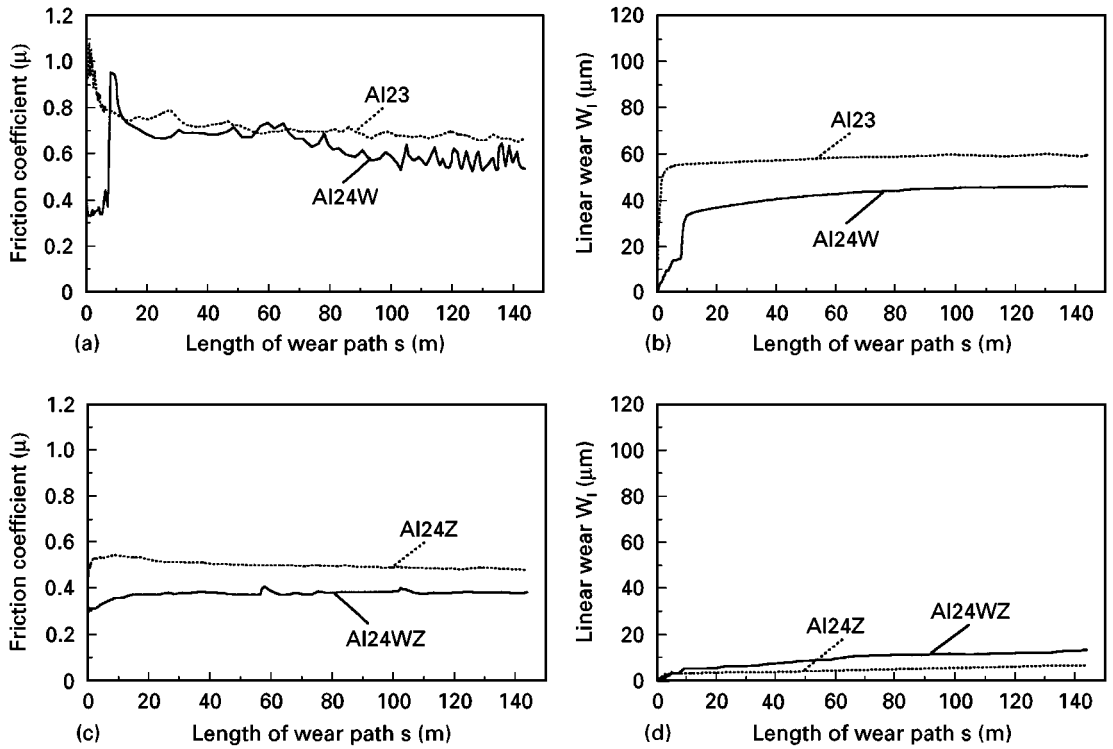

Figure 3 Friction coefficient of (a) Al223 and Al24W, and (c) Al24Z and Al24WZ, as well as the amount of linear wear W_l (sum of ball and block) of (b) Al23 and Al24W and (d) Al24Z and Al24WZ during oscillating sliding contact against Al_2O_3, balls at the normal load of 40 N and a relative humidity of 50% versus length of wear path.

after 60–100 m sliding. Fig. 3b shows amount of linear wear, W_l (sum of ball and block wear), of the sliding pairs Al_2O_3 /Al23 and Al_2O_3/Al24W as a function of length of wear path. High values of friction coefficient observed at the beginning of the tests (Fig. 3a) corresponded with high wear intensities (slope of the $W_l(s)$ curve). Owing to the ball-on-block geometry, surface pressure decreased with increasing amount of wear on the ball, which led to lower wear intensity at prolonged time of testing. Compared to the self-mated alumina Al_2O_3/Al23, the amount of wear was by about 20% lower on the sliding pair with the tungsten-containing ceramic Al24W at the end of the tests.

Substantially lower values of friction coefficient and markedly reduced periods of running-in were measured on the ceramics Al24Z or Al24WZ (Fig. 3c). While the average value of quasi-stationary friction coefficient was about 0.5 for the zirconia-alloyed ceramic Al24Z mated to an Al_2O_3 ball, an additional reduction was achieved for the tungsten laser-dispersed ceramic Al24WZ which led to quasi-stationary friction coefficients between 0.36 and 0.4. Fig. 3d shows that the sliding pairs Al_2O_3/Al24Z and Al_2O_3/ Al24WZ resulted in 75%–85% lower amount of linear wear than the reference pair Al_2O_3/A123.

Fig. 4 shows scanning electron micrographs of surfaces of the ceramic Al23 and the laser-modified ceramics worn during oscillating sliding contact against Al_2O_3 balls over a sliding distance of 144 m. The worn surface of the reference ceramic Al23 (Fig. 4a) was covered with a partially cracked layer consisting of densified wear debris and loose wear particles. Those surface layers were also found on the worn ceramic Al24W (Fig. 4b) locally, but beside smooth and rather polished regions without wear damage owing to failure of the alumina matrix or pull-out of tungsten dispersoids. Compared with these both ceramics, worn surfaces of the composites Al24Z

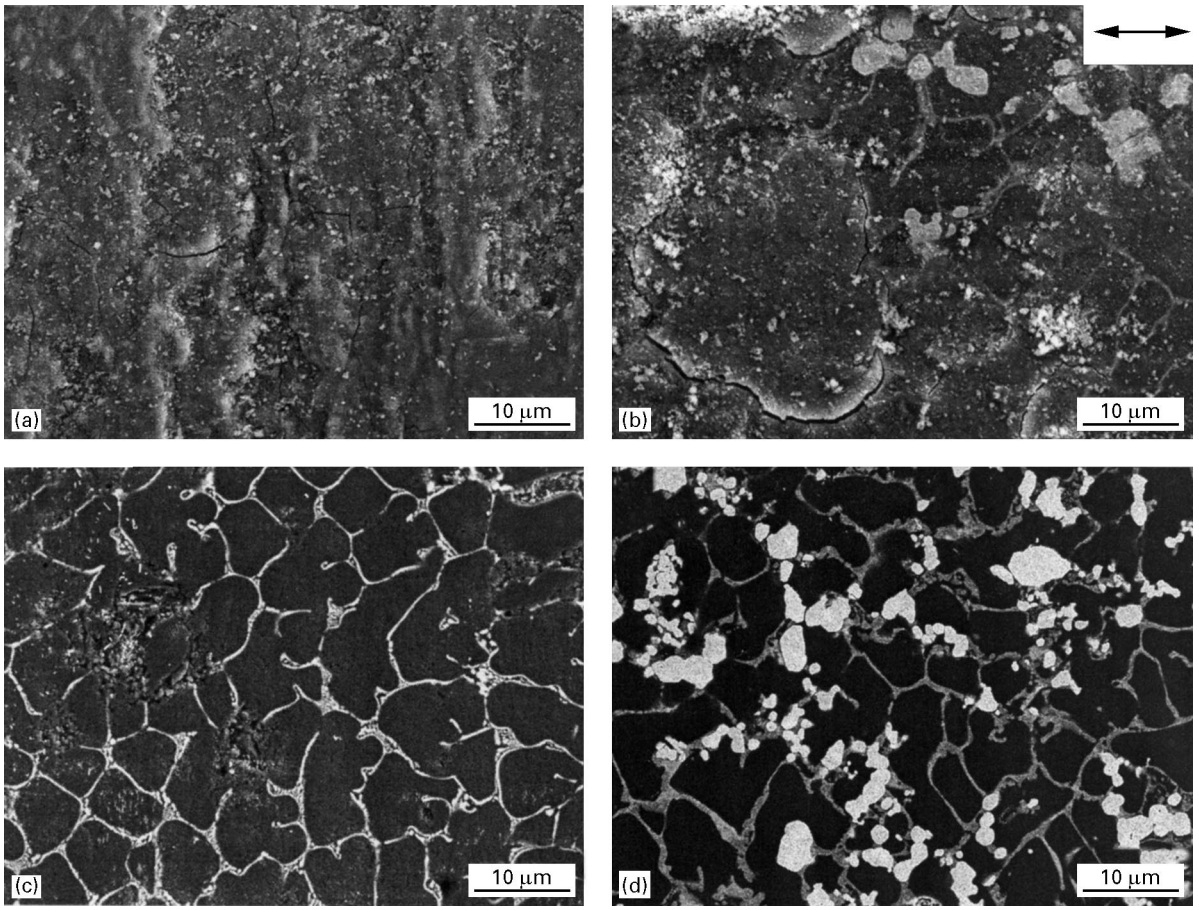

Figure 4 Scanning electron micrographs of surfaces of (a) Al23, (b) Al24W, (c) Al24Z and (d) Al24WZ worn during oscillating sliding contact against Al_2O_3 balls over a sliding distance of 144 m at the normal load of 40 N at relative humidity of 50% (arrow indicates sliding direction).

and Al24WZ (Fig. 4c and d) mated to alumina balls were smooth and polished, so that the alumina matrix, grain-boundary phase and tungsten dispersoids were clearly visible. Small areas of damage owing to failure of the grain-boundary phase occurred on the worn ceramic Al24Z, and also rolled-up tribochemical reaction films, probably consisting of aluminium hydroxide.

3.2.2. Effect of relative humidity

Fig. 5 shows the friction coefficient and amount of linear wear of the sliding pairs Al_2O_3/Al23 and Al_2O_3/Al24WZ at different relative humidities (3%, 30%, 80%) and in the presence of distilled water in the contact area. At a relative humidity of 3% (Fig. 5a), the friction coefficient of the sliding pair Al_2O_3/Al23 increased to a value of 0.9 immediately after starting the test, and reached a quasi-stationary value of 1.1 at prolonged time of testing. The high friction coefficient corresponded with a high wear intensity (slope of the $W_l(s)$ curve) initially, until the contact pressure was lowered due to wear of the Al_2O_3 ball after about 60 m sliding (Fig. 5b). Increasing the relative humidity led to a lower friction coefficient and amount of linear wear of the self-mated alumina after 144 m sliding. The lowest friction coefficient and amount of linear wear were measured in the presence of distilled water in the contact area. Compared with tests in dry air (3% RH), the quasi-stationary friction coefficient dropped to a value of 0.45 and the amount of linear wear by a factor of 13.

According to Fig. 5c and d, the sliding pair Al_2O_3/Al24WZ showed substantially lower friction coefficient and amount of linear wear than the pair Al_2O_3/Al23 at a given relative humidity. In dry air, Al_2O_3/Al24WZ exhibited an about 25% smaller quasi-stationary friction coefficient and only 50% of the amount of linear wear of the self-mated alumina after a length of wear path of 144 m. A relative humidity of 80% or distilled water in the contact area led to a low friction coefficient between 0.3 and 0.4, but a slight increase of linear wear compared with tests at 50% (Fig. 3d).

Fig. 6 shows scanning electron micrographs of surfaces of the ceramics Al23 and Al24WZ worn during oscillating sliding contact against Al_2O_3 balls in dry air (3% RH) and distilled water, respectively. After a sliding distance of 144 m, the monolithic ceramic Al23 (Fig. 6a) displayed a thick and rough surface layer consisting of densified and/or loose wear particles. Smooth areas occurred on the worn surface of the ceramic Al24WZ (Fig. 6b), where tungsten was analysed using energy-dispersive X-ray spectroscopy. Distilled water in the contact area of the self-mated alumina ceramic Al_2O_3/Al23 (Fig. 6c), led to tribochemical reaction layers and small surface cracks with local spalling of individual alumina grains or

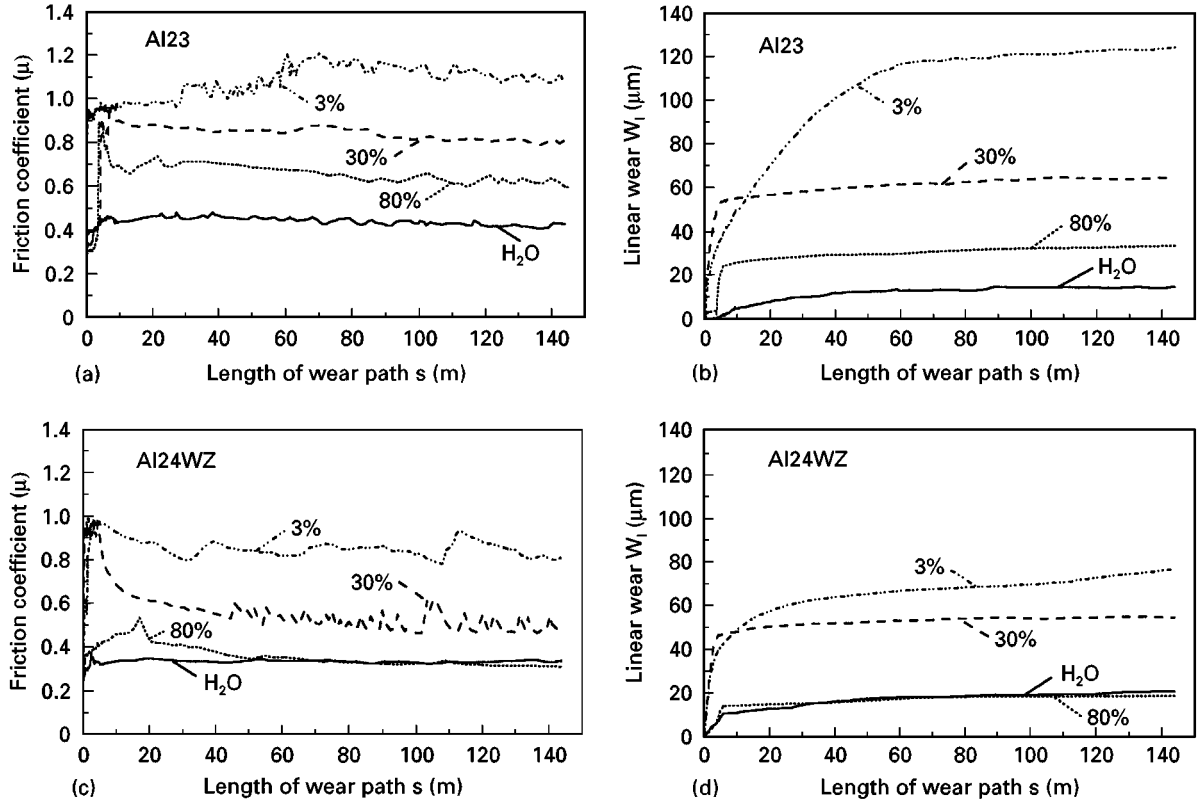

Figure 5 Friction coefficient of (a) Al23 and (c) Al24W, as well as amount of linear wear, W_1 of (b) Al23 and (d) Al24WZ during oscillating sliding contact against Al_2O_3 balls under the normal load of 40 N at relative humidities of 3%, 30%, 80% and the presence of distilled water versus length of wear path.

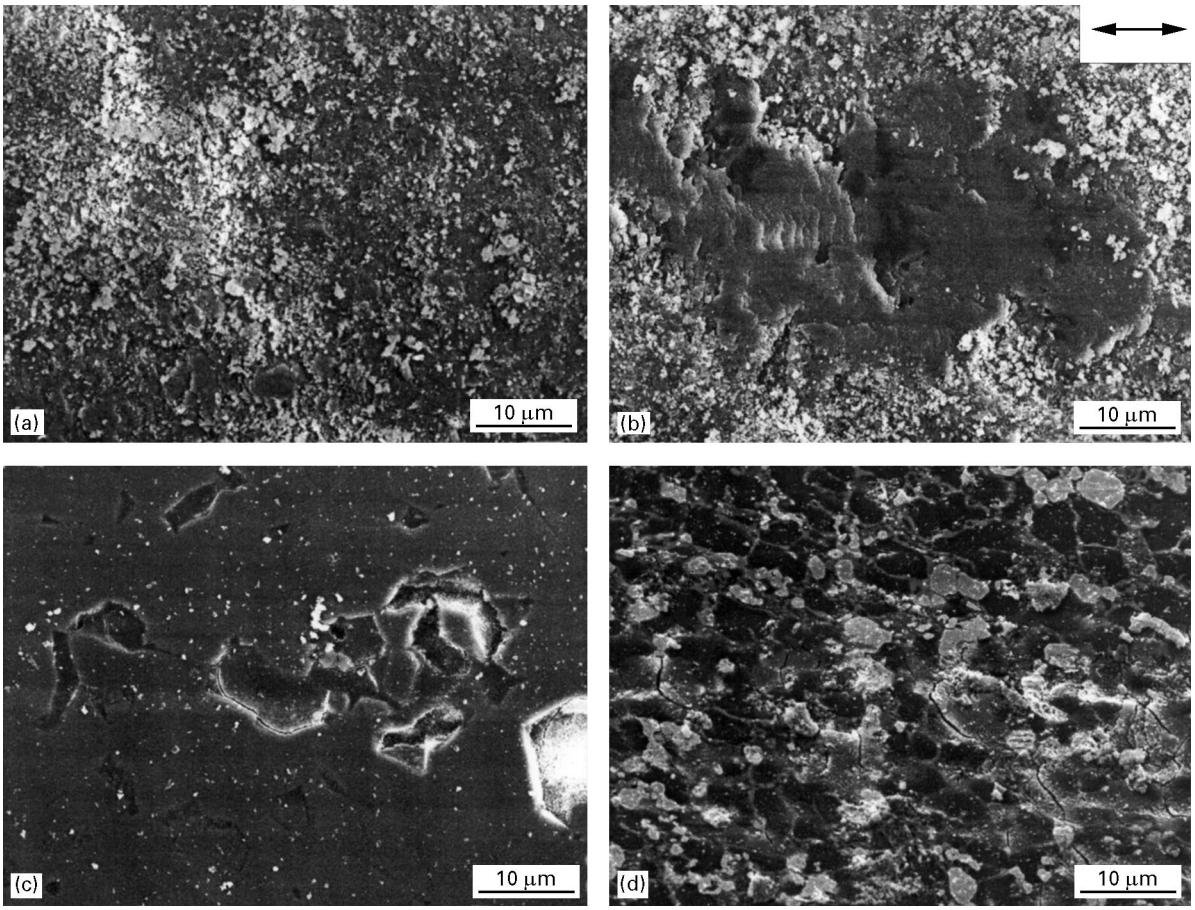

Figure 6 Scanning electron micrographs of surface (a, c) Al23 and (b, d) Al24WZ worn during oscillating sliding contact against Al_2O_3 balls over a sliding distance of 144 m under the normal load of 40 N and at (a, b) relative humidities of 3%, and (c, d) in the presence of distilled water (arrow indicates sliding direction).

parts of them. On the ceramic Al24WZ, the microstructure was visible after running the tribological test in the presence of distilled water (Fig. 6d), whereas it seemed that a thin layer covered the worn surface and small areas of densified wear particles occurred locally.

4. Discussion

The experimental results showed the substantially improved performance of tungsten laser-dispersed alumina ceramics compared with monolithic alumina ceramic under unlubricated oscillating sliding contact against Al_2O_3 counterbodies. Laser surface processing resulted in an almost dense multiphase microstructure (Al24WZ) containing tungsten dispersoids embedded in an alumina matrix, whereas a eutectic phase of Al_2O_3–ZrO_2 prevailed at the Al_2O_3 grain boundaries. Combination of tungsten and ZrO_2 additions led to distinctly smaller average grain size than that of the monolithic substrate ceramic Al24 (Table I). This agrees with results from the literature [7–9, 16], that ZrO_2 additions can reduce grain size during conventional sintering procedures as well as during laser alloying of alumina ceramic. Micrographs (Fig. 2) showed a homogeneous distribution of the tungsten particles owing to adequate convection in the alumina melt bath during laser processing and a good bonding to the alumina matrix after solidification. The results of the present study emphasized the distinct influence of the microstructure and relative humidity on friction and wear of the different multiphase surface layers. Fig. 7 summarizes the quasi-stationary values of friction coefficient and the amount of linear wear for the different ceramics mated to Al_2O_3 balls after a sliding distance of 144 m at relative humidities (RH) between 3% and 80% and in the presence of distilled water, respectively. At normal laboratory air of 50% RH, the lowest friction coefficient (Fig. 7a) was measured on the alumina ceramic with both tungsten and zirconia additions (Al24WZ). The friction coefficient was lower by more than 40% than that on the monolithic alumina ceramic (Al23) and was also lower than that on the zirconia-containing ceramic Al24Z, which underlies the beneficial effect of tungsten dispersoids with the ceramic Al24WZ.

The amount of linear wear, W_l^* (Fig. 7b) measured on surfaces of ball and block specimens using profilometry at the end of the tests, showed lower values for the laser-modified ceramics mated with alumina balls than the reference pair Al_2O_3/Al23. At a relative humidity of 50%, the amount of wear of the self-mated alumina (Al_2O_3/Al23) was distributed to about 60% on the Al23 block and 40% on the Al_2O_3 ball. Tungsten dispersoids in the ceramic Al24W reduced significantly the wear on the mated Al_2O_3 ball. Hence, it can

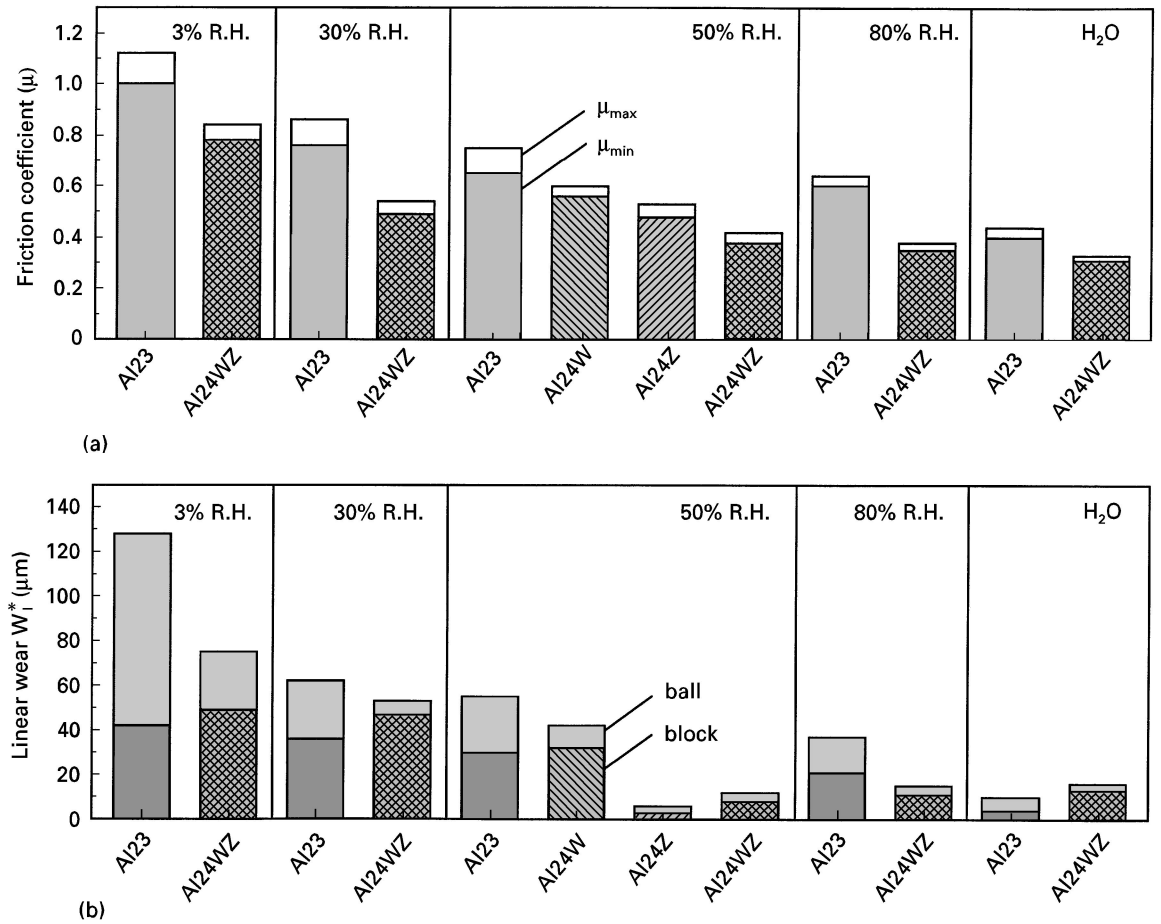

Figure 7 (a) Friction coefficient μ, and (b) amount of linear wear W_l^* of the different ceramics measured at the end or after a length of wear path of 144 m, respectively, under oscillating sliding contact against Al_2O_3 balls at the normal load of 40 N and at relative humidities of 3%, 30%, 50% and 80% (RH) as well as in the presence of distilled water.

be concluded that soft metallic particles caused milder damage on the Al_2O_3 balls and, with reference to Fig. 4b, a surface layer consisting of densified wear debris protected the contact surfaces. Fig. 7b shows further, that wear of the sliding pair Al_2O_3/Al24Z and Al_2O_3/Al24WZ had been reduced by a factor of 5–10 compared with the reference pair Al_2O_3/Al23. This was partially attributed to the reduced Young's modulus of the laser-modified ceramics and, as a result, to the reduced applied Hertzian pressure.

Wear tests were carried out on ball-on-block geometry, i.e. at the beginning of a test, a point contact prevailed theoretically between the mated solid surface, which changed into an area contact with increasing time and wear. Increasing wear led to a larger contact area and hence to a decreasing apparent contact pressure ($p = F_N/A$) at a constant normal load. Under the assumption that the apparent contact area, mainly determined by the amount of linear wear, W_1, of the ball specimen or the stroke during oscillating contact, is very small compared with the diameter, D, of the ball, the area of the contact $A(s)$ as a function of the length s of the wear path is given by [8]

$$A(s) = \pi[D - W_1(s)]W_1(s) \quad (1)$$

In Fig. 8 the instantaneous wear intensity as the slope of the $W_1(s)$ curve is plotted for the different ceramics over the instantaneous contact pressure calculated as the quotient of normal load and area $A(s)$. It became obvious that the pairs of both the monolithic alumina ceramic Al_2O_3/Al23 and the tungsten laser-dispersed ceramic Al_2O_3/Al24W showed high wear intensities under high contact pressure at the beginning of the tests. With increasing wear and hence decreasing contact pressure, wear intensity of both sliding pairs dropped rapidly by more than two orders of magnitude when the contact pressure fell below a critical value. At high contact pressure, wear intensity of the pairs Al_2O_3/Al24WZ and Al_2O_3/Al24Z displayed lower values by one to two orders of magnitude and transition from high to lower wear intensity occurred at greater contact pressure, compared with the two other pairs. This means that the load-carrying capacity for a given wear intensity was substantially improved on the laser-modified ceramics Al24WZ and Al24Z, respectively, when mated against Al_2O_3 balls.

According to Fig. 4a and b showing surfaces at the end of the tests, i.e. at conditions resulting in low wear intensity, worn surfaces of the ceramics Al23 an Al24W were covered with surface layers consisting of densified wear debris, while Al24WZ and Al24Z showed only very small damage and rather polished surfaces. It can be concluded that at high wear intensity, the wear behaviour of Al_2O_3/Al23 and Al_2O_3/Al24W was controlled by the stability of the surface layers and by intercrystalline microfracture, resulting in spalling of Al_2O_3 grains which may have acted abrasively on ball and block specimens [4]. Both effects led to relatively high friction coefficients (Fig. 3a). At a critical contact pressure, the surface layers were quasi-plastically deformed and densified leading to transition from high to low wear intensity. Softer and smoother surface layers such as on the pair Al_2O_3/Al24W, resulted in a lower quasi-stationary friction coefficient than that of the pair Al_2O_3/Al23.

The laser-modified ceramics Al24WZ and Al24Z exhibited lower sensitivity to contact pressure (Fig. 8) and under the experimental conditions used, microfracture and spalling of grains or tungsten dispersoids, respectively, did not occur. Alloying additions, such as tungsten or zirconia, to the alumina ceramic Al24 led to a distinctly lower value of Young's modulus compared with the monolithic ceramic Al23 (Table II). As a result, the maximum Hertzian contact pressure for ball-on-block geometry at the beginning of the tribological test was reduced from 1502 MPa (Al23), 1477 MPa (Al24Z), 1315 MPa (Al24W) to 1286 MPa (Al24WZ), when mating these ceramics to Al_2O_3 balls

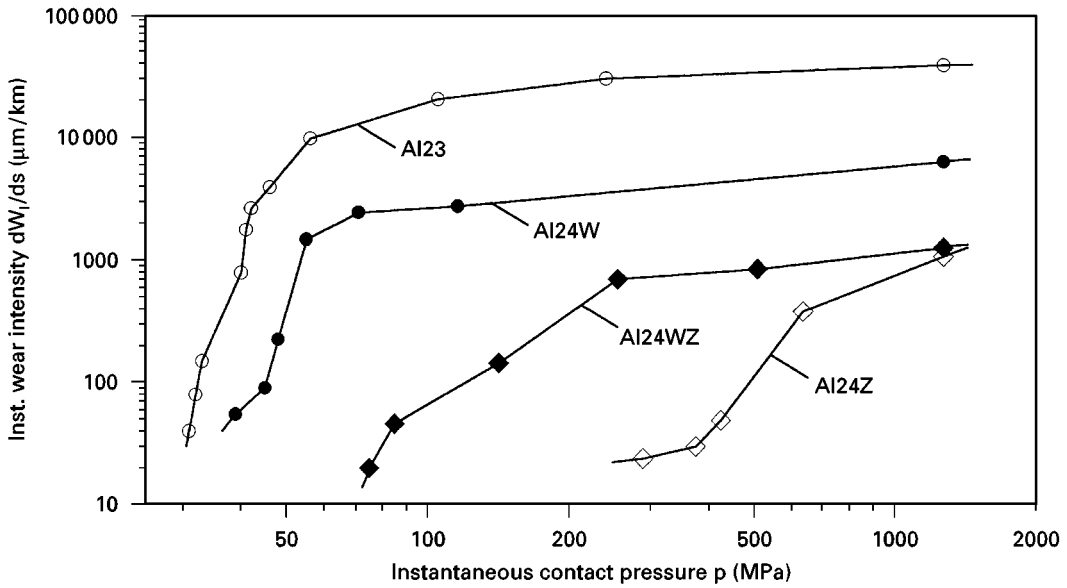

Figure 8 Instantaneous wear intensity dW_1/ds of the different ceramic pairs (A_2O_3 balls mated to Al23, Al24W, Al24WZ and Al24Z) during oscillating sliding at the normal load of 40 N and at a relative humidity of 50% versus calculated instantaneous contact pressure, p.

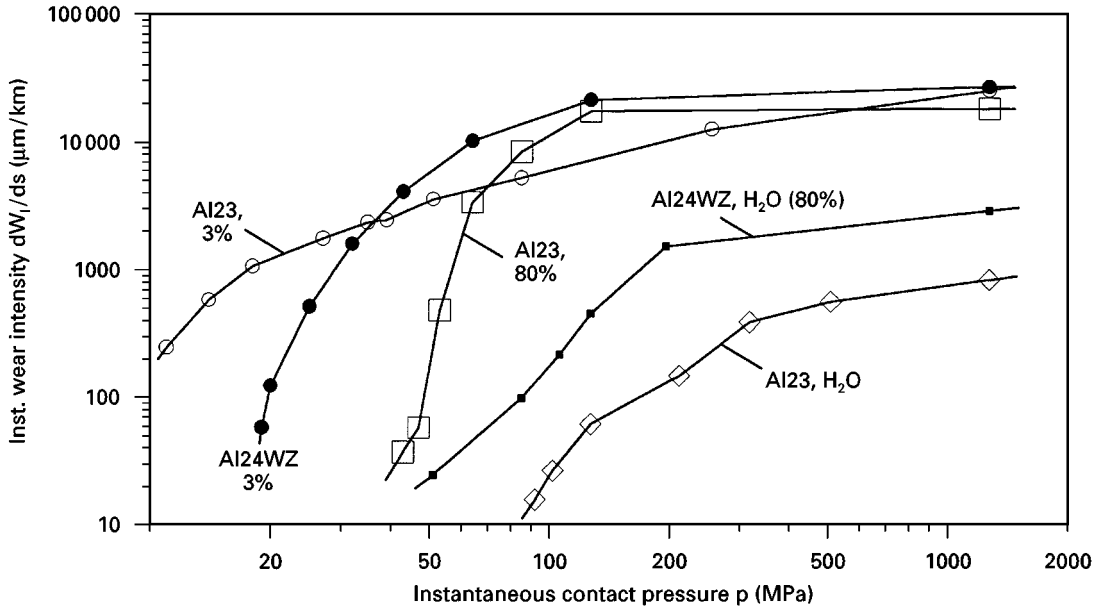

Figure 9 Instantaneous wear intensity dW_i/ds of the pairs Al_2O_3/ Al23 and Al_2O_3/Al24WZ during oscillating sliding at the normal load of 40 N and at relative humidities of 3% and 80% as well as in the presence of distilled water versus calculated instantaneous contact pressure, p.

(F 99.7) at the normal load of 40 N. This difference could also contribute to the relatively high ratio of wear on the ball to wear on the block for the pair Al_2O_3/Al23 (Fig. 7b).

According to Zum Gahr [6], the critical contact pressure for wear transition can be enhanced by increasing the fracture toughness and hardness or decreasing Young's modulus, friction coefficient and size of microstructural defects such as weak grain boundaries, pores, microcracks, etc., respectively. The hardness of the laser-modified ceramics was reduced by the incorporation of soft tungsten dispersoids and the Al_2O_3–ZrO_2 phase at grain boundaries (Table II, Fig. 4). On the other hand, an increase of fracture toughness was achieved due to the grain-boundary phase and processes of energy dissipation such as interactions of cracks with the tungsten dispersoids. Further, the laser-modified ceramics showed lower Young's modulus resulting in reduced applied contact pressure, and grain refinement as well as strengthening of grain boundaries could increase wear resistance, as reported for monolithic and laser-alloyed alumina ceramics [4, 5, 9]. Tribochemical reaction films could be formed during sliding contact on the smooth surfaces of Al24Z and Al24WZ (Fig. 4) owing to avoidance of microfracture. A low shear strength of tribochemical reaction films such as aluminium hydroxide was reported on self-mated alumina ceramic at different relative humidities [17]. In the present study, the lower friction coefficient of Al_2O_3/Al24WZ in comparison to Al_2O_3/Al24Z supports the conclusion that the tribochemical induced formation of tungsten oxides acted beneficially on friction in addition to aluminium hydroxide. In other investigations [18], a low friction coefficient was measured when alumina ceramic was mated to a ball of cemented carbides (WC6Co) and this was explained by thin tribochemical reaction layers (perhaps WO_3) formed in the tribological contact.

Fig. 9 shows the influence of relative humidity on wear intensity and wear transition for the sliding pairs Al_2O_3/Al23 and Al_2O_3/Al24WZ, respectively. Tribological performance of the monolithic alumina ceramic depended obviously more sensitively on relative humidity than the pair with the multiphase alumina ceramic Al24WZ. At high applied contact pressure, wear intensity of the pair Al_2O_3/Al23 was nearly independent of humidity but the critical contact pressure for wear transition was shifted to lower values in dry air (3%). Compared to 80% RH, the wear transition was shifted to a higher contact pressure in the presence of distilled water due to tribochemical reaction layers occurring in the contact area (Fig. 6c). Wear intensity of the pair Al_2O_3/Al24WZ at high applied contact pressure was reduced by more than one order of magnitude and wear transition was shifted to substantially higher contact pressure when humidity was changed from 3% to 80% or in the presence of H_2O. No difference was measured between the data at 80% and in distilled water, respectively. At a high humidity of 80%, the tribological performance of the pair Al_2O_3/Al24WZ was more favourable than that of Al_2O_3/Al23. However, wear intensity was substantially lower for Al_2O_3/Al23 when distilled water was present in the contact area. In dry air (3% RH), large damage occurred on the contact surfaces of both ceramics owing to microfracture processes, while tribochemical-induced formation of interfacial films dominated wear at high humidities or distilled water. From the results, it seems that distilled water reduced the wear intensity on the pure alumina Al23 more effectively than on the tungsten dispersoids containing Al24WZ.

5. Conclusion

Laser-induced incorporation of tungsten particles into an alumina matrix and/or laser-alloying of alumina

with zirconia resulted in multiphase surface structures of a thickness up to 800 μm showing substantially improved tribological performance during unlubricated oscillating sliding wear against Al_2O_3 balls. Grain refinement, strengthening of the grain boundaries by a eutectic Al_2O–ZrO_2 phase and soft tungsten dispersoids embedded in the Al_2O_3 matrix led to lower hardness and Young's modulus as well as higher fracture toughness of the laser-modified ceramic Al24WZ compared with a commercial alumina ceramic Al23 used for reference. Sliding pairs of the modified ceramic Al24WZ mated to Al_2O_3 counterbodies showed a friction coefficient lower by almost 50%, and lower linear wear by a factor of about 5 and a substantially higher value of the critical contact pressure for transition from low to high wear. Under conditions of severe wear, the contact surface of the laser-modified alumina was protected by surface layers of densified wear debris, while tribochemically induced surface layers dominated tribological behaviour in the mild wear regime.

References

1. S. JAHANMIR and X. DONG, in "Friction and wear of ceramics" (Dekker, New York, 1994) pp. 15–49.
2. S. M. HSU and M. G. SHEN, *Wear* **200** (1996) 154.
3. K. ADACHI, K. KATO and N. CHEN, *ibid.* **203–204** (1997) 291.
4. K.H. ZUM GAHR, W. BUNDSCHUH and B. ZIMMERLIN, *ibid.* **162–164** (1993) 269.
5. O. O. AJAYI and K. C. LUDEMA, *ibid.* **154** (1992) 371.
6. K.-H. ZUM GAHR, *ibid.* **200** (1996) 215.
7. S.-Z. LEE and K.-H. ZUM GAHAR, *Ceram. Int.* **20** (1994) 147.
8. K.-H. ZUM GAHR, C. BOGDANOW and J. SCHNEIDER, *Wear* **181–183** (1995) 118.
9. K. PRZEMECK and K.-H. ZUM GAHR, *Kermai. Z.* **49** (1997) 97.
10. L. S. SIGL, P. A. MATAGA, B. J. DALGLEISH, R. M. McMEEKING and A. G. EVANS, *Acta Metall.* **36** (1988) 945.
11. A. G. EVANS, *J. Am. Ceram. Soc.* **73** (1990) 187.
12. J. WANG, C. B. PONTON and P. M. MARQUIS, *Br. Ceram. Trans.* **92** (1993) 67.
13. X. SUN and J. YEOMANS, *J. Am. Ceram. Soc.* **79** (1996) 2705.
14. A. G EVANS and E. A. CHARLES, *ibid.* **59** (1976) 371.
15. M. F. DOERNER and W. D. NIX, *J. Mater. Res.* **1** (1986) 601.
16. J.-T. LIN and H.-Y. LU, *Ceram. Int.* **14** (1988) 251.
17. M. G. GEE, *Wear* **153** (1992) 201.
18. K.-H. ZUM GAHR and J. SCHNEIDER, in Proceedings of the International Tribological Conference, Yokohama, Japan (1996) pp. 397–402.

Received 16 December 1997
and accepted 15 May 1998